Optimum single gap solar cells for missions to Mercury

E. López[1*], A. Martí[1†]

[1]*Instituto de Energía Solar – Universidad Politécnica de Madrid ETSI Telecomunicación, Ciudad Universitaria sn 28040 Madrid, Spain*

J. M. Llorens[2‡], J. Buencuerpo[2§]

[2]*IMM-Instituto de Microelectrónica de Madrid (CNM-CSIC), Isaac Newton 8, PTM, E-28760 Tres Cantos, Madrid, Spain*

T. Versloot[3**]

[3]*Advanced Concepts Team, European Space Research and Technology Centre, Keplerlaan 1, 2201 AZ Noordwijk, The Netherlands*

Nomenclature

A = Solar array area, m^{-2}

B = Spectral radiance, $W \cdot sr^{-1} \cdot m^{-2}$

c = Speed of light, $m \cdot s^{-1}$

D = Altitude of polar orbit around Mercury, km

D_M = Orbit of Mercury around the Sun, km

E_{Fe} = Quasi-Fermi level of electrons, eV

E_{Fh} = Quasi-Fermi level of holes, eV

[*]PhD student, Instituto de Energía Solar, ETSI Telecomunicación, Universidad Politécnica de Madrid, 28040 Madrid, Spain; esther.lopez@ies-def.upm.es.
[†]Professor, Instituto de Energía Solar, ETSI Telecomunicación, Universidad Politécnica de Madrid, 28040 Madrid, Spain; amarti@etsit.upm.es.
‡Internal Research Scientist, IMM-Instituto de Microelectrónica de Madrid, Isaac Newton 8, PTM, E-28760 Tres Cantos, Madrid, Spain; jose.llorens@imm.cnm.csic.es.
[§]PhD student, IMM-Instituto de Microelectrónica de Madrid, Isaac Newton 8, PTM, E-28760 Tres Cantos, Madrid, Spain; jeronimo.buencuerpo@imm.cnm.csic.es.
** Internal Research Scientist, Advanced Concepts Team, European Space Research and Technology Centre, Keplerlaan 1, 2201 AZ Noordwijk, The Netherlands; Thijs.Versloot@esa.int.

E_G = Bandgap energy, eV

h = Planck's constant, J·s

H = Etendue, m^2·sr

k_B = Boltzmann's constant, $J \cdot K^{-1}$

L = Radiance emitted from a black body, $W \cdot sr^{-1} \cdot m^{-2}$

$\dot{N}$ = Photon's flux, s^{-1}

P_{INb} = Power radiation absorbed by the back side, W

P_{INf} = Power radiation absorbed by the front side, W

P_M = Power radiation emitted by Mercury, W

P_R = Power radiation reflected by Mercury, W

P_S = Power radiation from the Sun, W

R = Reflectivity

R_M = Radio of Mercury, km

R_S = Radio of the Sun, km

T_{M1} = Temperature of Mercury's surface facing the Sun, K

T_{M2} = Temperature of Mercury's surface not facing the Sun, K

T_{opr} = Operating temperature, K

T_S = Temperature of the Sun, K

x = Aluminum content

η = Limiting efficiency

θ_M = Subtended angles of Mercury, rad

θ_S = Subtended angles of the Sun, rad

μ = Chemical potential, eV

σ = Stefan-Boltzmann constant, $W \cdot m^{-2} \cdot K^{-4}$

Introduction

The power supply for space probes is usually based on photovoltaic (PV) systems. The first solar cells used in these systems were single-gap solar cells fabricated with Si and GaAs. Later on, multi-junction solar cells based

(MJSC) on III-V semiconductors were developed because of their higher efficiency and tolerance to a radiation environment [1]. All these solar cells have been based on semiconductors that fulfill the needs of most near-Earth missions. However, those same semiconductors fail to meet the needs of some other missions involving harsh environments such as high intensity high temperature (HIHT) environments [2]. In this work we investigate which semiconductor material is optimum to implement single gap solar cells for missions to Mercury where HIHT conditions are expected.

Since solar cell efficiency decreases as temperature increases [3], achieving high efficiency photovoltaic conversion at HIHT conditions is a big challenge. Previous works have pointed out the need of using wide-bandgaps semiconductors to reach this goal [4],[5]. In this context, we will study the potential of solar cells based on $Al_xGa_{1-x}As$, a well-known semiconductor whose physical properties have been deeply investigated. The limiting efficiency of these solar cells performing in near Mercury missions will be calculated to determine the optimum composition for $Al_xGa_{1-x}As$.

Theoretical model

The photovoltaic conversion efficiency of solar cells is maximized if carriers recombine only by emitting photons. In this context, detailed balance becomes the suitable theoretical model to determine the limiting efficiency of solar cells [6]. The application of detailed balance demands, in addition to the knowledge of the bandgap of the semiconductor the solar cell is made of, of the knowledge of the incident radiation (P_{IN}) and the temperature of operation of the solar cells (T_{opr}). These two parameters depend on the features of the space mission and the PV system respectively. Therefore, the starting point of our work will be to contextualize the problem and to establish a method to find out the value of these parameters.

We will study the case of PV arrays that describe polar orbits around Mercury while they face the Sun, as depicted in Fig.1 (a). In this kind of orbits, solar cells operate under the same conditions when they are situated at any point of the orbit. They receive not only the power radiation that comes from the sun (P_S), but also the power radiation emitted and reflected by Mercury, P_M and P_R respectively. These power radiations reach the solar array with different solid angles, which, particularly in the case of P_M and P_R depend on the orbit described by the satellite. It is important to take into account the contribution of Mercury to the total power radiance since for the case of polar orbits close to the

planet, it may represent around 38% of the total radiation received, as discussed later. Other power radiations received by PV arrays, such as the 3K cosmic background radiance [7] or the power radiation from other bodies in the solar system, will be considered negligible.

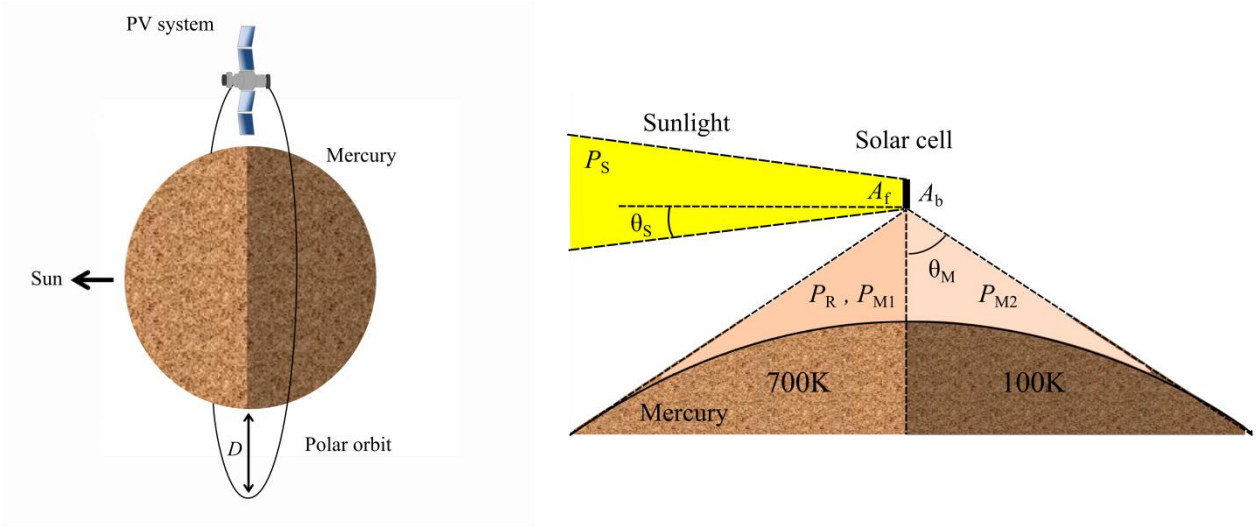

(a) (b)

Fig. 1. (a) Sketch of the polar orbits around Mercury that are studied in this work. (b) Side view of the different power radiations received by the solar cells.

When the radiations are approximated by black body radiation (as it will be our case) these radiations can be obtained from the Stephan-Boltzmann law, which describes the radiance, L ($W \cdot sr^{-1} \cdot m^{-2}$), emitted from a black body in terms of its temperature. While the temperature of the Sun can be considered homogeneous at 5771K (which is in agreement with the value of the solar constant at Earth, $1366.11 W/m^2$), the temperature of Mercury cannot. In this planet there is a high thermal gradient as consequence of the absence of atmosphere [8]. For simplification, we will consider that the temperature of the half part of Mercury that faces the Sun is 700 K (T_{M1}), and the temperature of the other half is 100 K (T_{M2}). Besides, we will consider that this planet has a Lambertian surface with a reflectivity (or albedo), R (equal to 0.1 [9]), and in consequence, with an emissivity (1-R).

The power absorbed by the area of the front side (A_f) and the back side (A_b) of the PV array, will be obtained by multiplying, respectively, the radiances impinging on the front and the back side of the array by its corresponding etendues, H. The radiance, L ($W \cdot sr^{-1} \cdot m^{-2}$), and the etendue, H ($sr \cdot m^2$), are given respectively by:

$$L = \varepsilon \frac{\sigma \cdot T^4}{\pi} \tag{1}$$

$$H = \frac{1}{2} \cdot (sin\theta)^2 \cdot \varphi \cdot A \tag{2}$$

where σ is the Stefan-Boltzmann constant ($5.67 \cdot 10^{-8}$ $W \cdot m^{-2} \cdot K^{-4}$), ε and T are respectively the emissivity and the temperature of the body that emit the radiation, and θ is the subtended angle by this radiation. In equation (2), φ is 2π for the radiation coming from the Sun and π for the radiation coming from Mercury. In this equation the etendue is calculated assuming that the size of *A* is irrelevant, which is a good approximation in the given context, so:

$$P_{Sf} = H_S . L_S = \pi \cdot (sin\theta_S)^2 \cdot A_f \cdot \frac{\sigma \cdot T_S^4}{\pi} \tag{3}$$

$$P_{Rf} = H_R \cdot L_R = \frac{\pi}{2} \cdot (sin\theta_M)^2 \cdot A_f \cdot R \cdot (sin\theta_S)^2 \cdot \sigma \cdot T_S^4 \tag{4}$$

$$P_{M1f} = H_{M1f} \cdot L_{M1} = \frac{\pi}{2} \cdot (sin\theta_M)^2 \cdot A_f \cdot (1 - R) \cdot \frac{\sigma \cdot T_{M1}^4}{\pi} \tag{5}$$

$$P_{M2b} = H_{M2b} \cdot L_{M2} = \frac{\pi}{2} \cdot (sin\theta_M)^2 \cdot A_b \cdot (1 - R) \cdot \frac{\sigma \cdot T_{M2}^4}{\pi} \tag{6}$$

$$P_{INf} = P_{Sf} + P_{Rf} + P_{M1f} \tag{7}$$

$$P_{INb} = P_{M2b} \tag{8}$$

T_S is the temperatures of the Sun, and θ_S and θ_M are the subtended angles of the Sun and Mercury from the solar array respectively. The total power radiation absorbed by the front side and the back side of the PV array are P_{INf} and P_{INb} respectively.

Considering the size and the distance of the different elements:

$$\theta_S = atan\left(\frac{R_S}{D_M}\right) \tag{9}$$

$$\theta_M = asin\left(\frac{R_M}{R_M + D}\right) \tag{10}$$

R_S and R_M are the radius of the Sun and Mercury respectively, D_M is the orbit of Mercury around the Sun and D is the altitude of the polar orbit around Mercury. Data have been obtained from [10].

From the impact of P_{INf} and P_{INb} on the PV system, a high T_{opr} is expected. In order to minimize this temperature, a selective reflector should be used. Selective reflectors consist in material layers deposited on the surface of the solar cells which allow only photons of certain energy to reach the solar cell. In the ideal case, these photons are those ones that can be converted to electrical power, whose energy is higher than the bandgap (E_G). Below bandgap energy photons are therefore reflected back towards the light source [11].

Notice that, the use of selective reflectors implies that P_{INf} depends on E_G. This dependence cannot be described by equations (3)-(5). Therefore, in this case, it is necessary to use generalized Planck's law to calculate the spectral radiance. In this respect, equation (11) below gives the radiance according to this generalized law, for energies between E_1 and E_2, characterized by a chemical potential μ and temperature T.

$$B(E_1, E_2, \mu, T) = \frac{2}{h^3 c^2} \int_{E_1}^{E_2} \frac{E^3}{e^{\frac{E-\mu}{k_B \cdot T}} - 1} dE \tag{11}$$

In this equation h is the Planck constant ($6.626 \cdot 10^{-34}$ J·s), c is the speed of light ($2.998 \cdot 10^{8}$ m·s^{-1}) and k_B is the Boltzmann constant ($1.381 \cdot 10^{-23}$ J·K^{-1}). So, if selective reflectors are used, $B(E_G, \infty, 0, T)$ replaces $\frac{\sigma \cdot T^4}{\pi}$ in equations (3)-(5).

To determine the value of T_{opr}, it is necessary to establish a balance between the power absorbed, the electrical power produced and the power emitted. This balance takes into account that the electric power density (W) produced by the PV array depends on the temperature, the bandgap of the solar cells and the operation point (defined by the output voltage, V). Assuming all parts of the satellite system are in thermal equilibrium, T_{opr} can be obtained by solving the power balance equation (12).

$$P_{INf}(E_G) + P_{INb} - W(E_G, T_{opr}, V) \cdot A_f = \pi \cdot A_b \cdot \frac{\sigma \cdot T_{opr}^4}{\pi} + \pi \cdot A_f \cdot B(E_G, \infty, e \cdot V, T_{opr}) \tag{12}$$

According to this equation both surfaces, A_b and A_f, emit radiation. However, while emission from A_b corresponds to a black body, emission from A_f does not because, on one hand, this area corresponds to a surface covered with an

ideal selective reflector, which only emits photons whose energy is higher than E_G. On the other hand, these photons proceed from electron-hole pairs recombination processes and therefore, they are characterized by μ=e·V.

An important observation derived from equation (12) is that, solar cells with different bandgaps will operate at different T_{opr}. These temperatures are expected to be minimized when using ideal selective reflectors. However, this could be non-viable. Because of this, we shall study two scenarios: (a) that uses ideal selective reflectors and (b) that does not use selective reflectors. Notice that if selective reflectors are not used, photons with energies lower than E_G will be absorbed in the solar cells by free carriers or in the back contact. Consequently, the inverse process is possible and, in this case, A_f can emit photons whose energy is lower than E_G and μ=0. This modifies equation (12) as follows:

$$P_{INf} + P_{INb} - W\left(E_G, T_{opr}, V\right) \cdot A_f = \tag{13}$$

$$= \pi \cdot A_b \cdot \frac{\sigma \cdot T_{opr}^4}{\pi} + \pi \cdot A_f \cdot B\left(E_G, \infty, e \cdot V, T_{opr}\right) + \pi \cdot A_f \cdot B\left(0, E_G, 0, T_{opr}\right)$$

In both cases, the limiting efficiency is calculated by:

$$\eta = \frac{W\left(E_G, T_{opr}, V\right)}{P_{INf}(E_G = 0)} \tag{14}$$

where W is the maximum product between V and the current density, J, produced by solar cells. These data are obtained from the detailed balance, where the quasi-Fermi level of electrons and holes, E_{Fe} and E_{Fh} respectively, are considered flat so that.

$$E_{Fe} - E_{Fh} = \mu = e \cdot V \tag{15}$$

In the detailed balance model J is proportional to the difference between the flux of photons absorbed by the solar cell, and the flux of photons emitted by the solar cell. Defining $\dot{N}$ as:

$$\dot{N}(E_1, E_2, \mu, T) = \frac{2}{h^3 c^2} \int_{E_1}^{E_2} \frac{E^2}{e^{\frac{E-\mu}{k_B \cdot T}} - 1} dE \tag{16}$$

J can be obtained by equation (17) as follows:

$$J = e \cdot [\pi \cdot (sin\theta_S)^2 \cdot \dot{N}(E_G, \infty, 0, T_S) + \pi \cdot (1 - R) \cdot (sin\theta_M)^2 \cdot \dot{N}(E_G, \infty, 0, T_{M1})/2 + \quad (17)$$

$$+\pi \cdot R \cdot (sin\theta_M)^2 \cdot (sin\theta_S)^2 \cdot \dot{N}(E_G, \infty, 0, T_S)/2 - \pi \cdot \dot{N}\left(E_G, \infty, e \cdot V, T_{opr}\right)]$$

It is important to point out that E_G depends on the temperature, T, and the Al content, x, in $Al_xGa_{1-x}As$. Depending on x, $Al_xGa_{1-x}As$ can be a direct or indirect gap semiconductor.

Direct bandgaps lead to higher absorption coefficients, and, therefore, to the possibility of using thinner solar cells. This offers advantages such as, the reduction of weight and the reduction of photon absorption by free carriers when selective reflectors are not used. For these reasons, it is preferred that E_G correspond to the direct valley of the conduction band, E_Γ for which $Al_xGa_{1-x}As$ is a direct bandgap semiconductor [12].

$$E_G(x,T) = E_{\Gamma,0}(x) - 5.41 \cdot 10^{-4} \cdot \frac{T^2}{T + 204}\ (eV) \quad (18)$$

$$E_{\Gamma,0}(x) = 1.519 + 1.155x + 0.37x^2\ \ (eV) \quad (19)$$

Results

We have studied the range of composition $x \leq 0.4$ because, for this range, E_Γ is the lowest energy valley when $T_{opr} < 1000$ K. Fig.2 shows the limiting efficiencies for each limit case: (a) and (b).

The results have been calculated for two different altitudes of the polar orbit, D=200 km and D=15000 km. These values correspond to the lowest and the highest points of the eccentric orbit described by MESSENGER (the space mission to Mercury launched in 2004) [13]. The altitude of polar orbits impacts significantly on the value of the subtended angle by Mercury from the PV array (θ_M). As a consequence, the power radiation that the PV array receives from Mercury (P_M and P_R) at D=15,000 km is only 2.3% of the power radiation that the PV array receives from Mercury at D=200 km. At D=200 km, P_M and P_R comprise the 38.2% of the total P_{INf} absorbed by solar cells without ideal reflectors. However, when ideal reflectors are incorporated, P_M and P_R reduce their importance and comprise the 4.1% of the total P_{INf} (for an Al composition x =0.4). This fact is due to that, at D=200 km, the radiation received from Mercury is mostly formed by photon energies below the bandgap value, which are not absorbed by PV arrays covered with ideal reflectors. In particular, at D=200 km, 93% of the received radiation from Mercury corresponds to P_M, whose spectrum is that of a 700K black body (the radiation coming from the cold side of Mercury is negligible) and

7% corresponds to P_R, whose spectrum is that of a 5771K black body. Summarizing, different combinations between polar orbits (D=200 km and D=15000 km) and the incorporation or not of selective reflectors result in different values of P_{INf}. These values are used to calculate the limiting efficiency depicted in Fig. 2, where it is important to note that, higher W may not correspond to higher η.

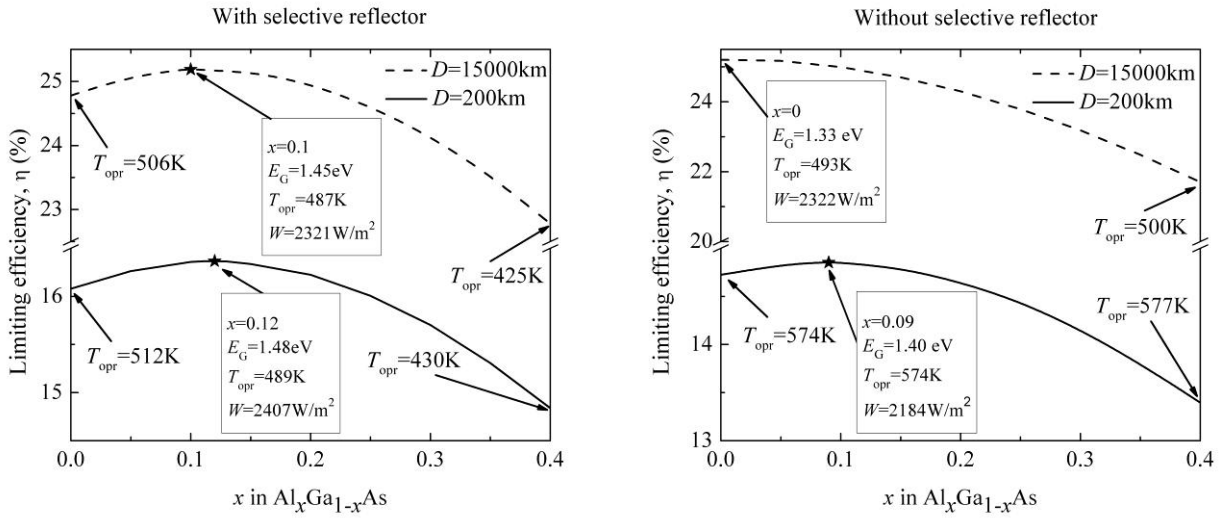

(a) (b)

Fig. 2. Limiting efficiency of solar cells based on $Al_xGa_{1-x}As$ with ideal selective reflectors (a) and without selective reflectors (b).

The data of Fig. 2 are obtained using the software "Wolfram Mathematica", imposing a precision of 50 significant digits during the computational processes.

Discussion

In each curve of Fig.2 (a) and (b) the optimum composition, x, to implement solar cells for Mercury's missions is taken as the one leading to the highest limiting efficiency. It can be noticed that, different operating conditions (in terms of the use of selective reflectors or not and height of the orbit described) lead to different optimum compositions.

When selective reflectors are used (Fig.2 (a)), the optimum composition is around x=0.11 and the limiting efficiencies are 16.4% and 25.2%, for D=200 km and D=15000 km respectively. In spite of these low limiting

efficiencies, the system can produce high electrical power densities (2321 W/m^2 – 2407 W/m^2) because of the high irradiances received by the PV system. Selective reflectors reflect photons whose energy is lower than the value of the bandgap, which only contribute to the heating the solar cells. In particular, at D=200km, the reflected radiation constitute the 69.6% of the radiation that reach the surface of the PV array and, at D=200km, it is the 53.4%. As a consequence, the use of selective reflectors reduces the operation temperatures to the 425–512 K range which, in practice, would lead to lower dopant diffusion and lower degradation rates of the metal contacts. An additional advantage is that the presence of these reflectors can reduce the exposure to the undesired high-radiation (electrons, protons, etc.), whose harmful effects are not analyzed in this work [14].

If selective reflectors are not used (Fig.2 (b)), the estimated T_{opr} increases its value to the 493–577 K range. Under these conditions, wide bandgap semiconductors, as $Al_xGa_{1-x}As$ are not optimum to implement solar cells for D=15000 km. This result might seem to contradict previous results in which wide bandgaps solar cells are optimum at high temperatures [5, 15], although, in fact, there is no such contradiction. The reason is that, in the model described in this work, the choice of different bandgaps also implies the solar cells operate at different T_{opr}. For example, when selective reflectors are used and D is 15000 km, increasing x from 0 to 0.4, produces a decrease in T_{opr} from 506 K to 425 K. In contrast, when selective reflectors are not used, increasing x from 0 to 0.4, produces an increase in T_{opr} from 493 to 500 K. In this case, x=0 is the optimum composition not because its gap (1.33 eV) is the optimum at 493 K, but because this gap leads to lower temperatures when compared to the temperatures of the bandgaps corresponding to x>0.

The values of these efficiencies (Fig.2) are theoretical upper limits, which will be not reached in practice. The efficiency of practical AlGaAs solar cells for Mercury's mission can be estimated on the basis of the empirical data we dispose today. In this sense, 19.2% efficient $Al_{0.2}Ga_{0.8}As$ solar cells have been reported (for AM2) [16]. This experimental value is 69% of the theoretical limiting efficiency of solar cells with the same composition, x=0.2 (27.7 % for AM0 and T_{opr}=300K). In spite of these data are not completely comparable because they are obtained under different spectrums (AM2 and AM0), we can use them to estimate that $Al_{0.11}Ga_{0.89}As$ solar cells (with selective reflectors) can achieve practical efficiency values of 11.3% and 17.4% for Mercury's orbits with D=200 km and D=15000 km respectively. These efficiencies could be increased if these single gap solar cells are used as part of multi-junction solar cells (MJSCs) as for example it has been the case of the GaAs/Ge solar cells designed for the

BepiColombo mission (the first European mission to the planet Mercury) [17]. In this mission, 104 and 5 GaAs/Ge solar cells are connected in series and parallel respectively, to form each solar panel of a total solar array of 55 m^2. This solar array can be tilted to limit the temperature to 473K and supply the power demand for the cruise to Mercury, which should be at least 10 kW at Earth's orbit. According to our calculus, the $Al_{0.11}Ga_{0.89}As$ single gap solar cells purposed in this work for Mercury's missions could guarantee this demand also, without the need of using the more complicated configurations of MJSC. This can be appreciated from Table I, where a comparison with data from GaAs/Ge solar cells is showed. To make this comparison possible, it has been assumed that the efficiency of the solar panel is 78% of the solar cell efficiency, which is extracted from [17]. So it is possible to extrapolate that, the same solar array used in BepiColombo with $Al_{0.11}Ga_{0.89}As$ single gap solar cells instead of GaAs/Ge solar cells would show efficiencies of 8.8%-13.6% for Mercury's orbits, and therefore, it could provide 68.7-71.2 kW.

	GaAs/Ge [17]	$Al_{0.11}Ga_{0.89}As$
Earth's orbit	*10.6 kW	11.6 kW
Mercury's orbit	*37 kW	68.7-71.2 kW

Table I: Comparison between the power generated by GaAs/Ge solar cells and $Al_{0.11}Ga_{0.89}As$ solar cells (with selective reflectors) at different orbits. *The array is tilted to limit the temperature to 473K.

During the first phase of the cruise to Mercury, the $Al_{0.11}Ga_{0.89}As$ single gap solar cells of this array would operate at temperatures between 300-286K (the lowest limit is calculated with the method described in this work, assuming the solar array is placed at Earth's orbit). Then, the solar array would present practical efficiencies of around 15.5%, and therefore, it could provide around 11.6 kW.

Conclusions

In Mercury's missions, solar cells should be covered by selective reflectors in order to operate at more viable temperatures. The optimum single gap solar cell is based on $Al_{0.11}Ga_{0.89}As$, whose limiting efficiency varies in the range of 16.4% – 25.2% along the eccentric orbit around Mercury. In spite of these low efficiencies, these solar cells could produce high power densities (2321 Wm-2 – 2407 Wm-2), due to the high intensity of the solar illumination that characterize these missions.

Acknowledgments

This work was supported by the European Space Agency contract No 4000112049/14/NL/MV under the GSP/ARIADNA program and the MADRID-PV Project granted by the Comunidad de Madrid (Contract S2013/MAE-2780).

References

[1] L. El Chaar, L. A. Lamont, and N. El Zein, "Review of photovoltaic technologies," *Renewable & Sustainable Energy Reviews*, vol. 15, pp. 2165-2175, Jun 2011.

[2] A. Luque and S. Hegedus, *Handbook of Photovoltaic Science and Engineering*: Wiley, 2003.

[3] J. C. C. Fan, "Theoretical temperature-dependence of solar-cell parameters," *Solar Cells*, vol. 17, pp. 309-315, Apr-May 1986.

[4] D. Merritt, S. Houlihan, R. P. Raffaelle, and G. A. Landis, "Wide-bandgap space solar cells," *IEEE*, 2005, pp. 552-555.

[5] D. A. Scheiman, G. A. Landis, and V. G. Weizer, "High-bandgap solar cells for near-Sun missions," in *Space Technology and Applications International Forum - 1999, Pts One and Two*. vol. 458 Melville: Amer Inst Physics, 1999, pp. 616-620.

[6] W. Shockley and H. J. Queisser, "Detailed balance limit of efficiency of p-n junction solar cells," *Journal of Applied Physics*, vol. 32, p. 510, 1961.

[7] P. S. Henry, "A simple description of the 3 k cosmic microwave background," *Science (New York, N.Y.)*, vol. 207, pp. 939-942, 1980.

[8] A. R. Vasavada, D. A. Paige, and S. E. Wood, "Near-Surface Temperatures on Mercury and the Moon and the Stability of Polar Ice Deposits," *Icarus*, vol. 141, pp. 179-193, 1999.

[9] W. J. Kaufmann and A. Fraknoi, *Instructor's Guide to Accompany Universe, Third Edition, by William J. Kaufmann, III*: W.H Freeman, 1991.

[10] http://nssdc.gsfc.nasa.gov/planetary/factsheet/mercuryfact.html., Accessed: 2015-10-27. (Archived by WebCite® at http://www.webcitation.org/6canjjn01).

[11] C. M. Maghanga, G. A. Niklasson, C. G. Granqvist, and M. Mwamburi, "Spectrally selective reflector surfaces for heat reduction in concentrator solar cells: modeling and applications of TiO2:Nb-based thin films," *Applied Optics*, vol. 50, pp. 3296-3302, 2011.

[12] M. Levinshtein, S. L. Rumyantsev, and M. Shur, *Handbook Series on Semiconductor Parameters: Ternary and quaternary A3B5 semiconductors*: World Scientific, 1999.

[13] http://messenger.jhuapl.edu/the_mission/orbit.html., Accessed: 2015-10-27. (Archived by WebCite® at http://www.webcitation.org/6canxBOyY).

[14] D. Wernham, "Optical coatings in space," in *Advances in Optical Thin Films IV*, Marseille, France, 2011, pp. 81680F-81680F-11.

[15] D. Merritt, S. Houlihan, R. P. Raffaelle and G. A. Landis, "Wide-bandgap space solar cells," in *Conference Record of the Thirty-First IEEE Photovoltaic Specialists Conference - 2005*, 2005, pp. 552-555.

[16] G. F. Virshup, C. W. Ford, and J. G. Werthen, "A 19% efficient AlGaAs solar cell with graded band gap," *Applied Physics Letters*, vol. 47, pp. 1319-1321, 1985.

[17] http://www.sciops.esa.int/SB-general/Projects/BepiColombo-OLD/BepiColomboSTRep/Chapter6fin.pdf., Accessed: 2015-10-27. (Archived by WebCite® at http://www.webcitation.org/6cavhVtlm**)**.